≪Research Paper≫ Applied Science and Convergence Technology Vol.24 No.4, July 2015, pp.111～116
http://dx.doi.org/10.5757/ASCT.2015.24.4.111

Direct Comparison of Optical Properties from Graphene Oxide Quantum Dots and Graphene Oxide

Min-Ho Jang[a], Hyun Dong Ha[b], Tae Seok Seo[b], and Yong-Hoon Cho[a]*

[a]*Department of Physics and Graphene Research Center of KI for the NanoCentury, Korea Advanced Institute of Science and Technology, Daejeon 305-701, Korea*
[b]*Department of Chemical and Biomolecular Engineering and Institute for the BioCentury, Korea Advanced Institute of Science and Technology, Daejeon 305-701, Korea*

(Received July 22, 2015, Accepted July 29, 2015)

The graphene oxide (GO) and graphene oxide quantum dots (GOQDs), which have gained research interest as new types of light-emitting materials, were synthesized by the modified Hummers method for oxidation of graphite flake and graphite nanoparticle. The optical properties of GO and GOQDs have been compared by mean of photoluminescence (PL), PL excitation (PLE), UV-vis absorbance, and time-resolved PL. The GO have an absorption peak at 229 nm and shoulder part at 310 nm, whereas the GOQDs show broad absorption with a gradual change up without any absorption peaks. The PL emission of GOQDs and GO showed the green color at 520 nm and the red color at 690 nm, respectively. The red emission of GO showed faster PL decay time than the green emission of GOQDs. In particular, the temporal PL profile of the GO showed redshift from 560 nm to 660 nm after the pump event.

Keywords : Graphene oxide, Graphene quantum dot, Graphene oxide quantum dot, Photoluminescence, Time-resolved photoluminescence

I. Introduction

In recent years, the graphene have been intensively investigated because of their extraordinary properties, such as high carrier mobility, high transmittance, and excellent thermal and electrical conductivity [1]. These properties of the graphene lead to the most promising next-generation material of widespread technological applications. However, since graphene is a semi-metal with zero-band gap, observing photoluminescence (PL) from them is regarded as impossible. Nevertheless, opening a band gap could be introduced by reducing the lateral diameter of graphene and by functionalizing other atoms on graphene. In particular, the PL from graphene's derivative has been demonstrated. Gokus et al. observed the luminescence from graphene oxide (GO) by oxygen plasma treatment [2]. The GO is a single layer sheet with oxygen functional groups on the basal plane and/or at the edges. Pan et al. demonstrated the graphene quantum dots (GQDs) with strong blue emission by hydrothermal methods

* [E-mail] yhc@kaist.ac.kr

[3]. The GQDs are defined as the graphene with smaller diameter than 100 nm. Compared to fluorescent dye and colloidal semiconductor quantum dots, GO and GQDs have many advantages with cost-effectiveness for their synthesis, low toxicity, excellent solubility, stable PL, broad range of absorption [4,5]. Because of these features, they have gained giant interest as the new types of light-emitting material and have possibility to be applied for optoelectronics, molecular sensors and cellular bio-imaging.

Up to now, it is considered that the GQDs exhibit much stronger PL features than that of the GO. Their luminescence origins have not only same features in term of oxygen-functional groups and isolated sp^2 carbon domain in the sp^3 matrix but also different properties of size, shape, and edge effect [6-11]. Although there are many studies of GO and GQDs, there is lack of comparison between the optical properties of GO and GQDs. Herein, we prepared both samples of nano-sized graphene oxide quantum dots (GOQDs) and micro-sized GO by oxidizing different starting materials of graphite nanoparticles (GNPs) with 4 nm and graphite flake, respectively. Their optical properties were compared by means of PL, PL excitation (PLE), UV-vis absorbance, and time-resolved PL. The green PL emitting GOQDs and the red PL emitting GO were observed. The red emission of GO showed fast PL decay time than the green emission of GOQDs. This will provide important insights for understanding the optical properties in nano-scale GOQDs and micron-scale GO.

II. Experimental

The synthesis of GO and GOQDs has been reported elsewhere [9,12,13]. Briefly, graphite flakes (Sigma-Aldrich) and graphite nanoparticle (Scientific Industries, USA) were used as starting materials for GO and GOQDs, respectively. We employed the modified Hummers method for oxidation of starting materials. All of the data were obtained under room temperature and precision cells made of Suprasil quartz were used as a container for each sample during the optical measurements. The absorption properties were detected on a UV-vis spectrophotometer (S-3100, SCINCO, Korea). For the PL measurement, we selected a monochromatic light from a 300 W-xenon lamp as an excitation source, and for the detection, a UV spectrometer (Maya2000, Ocean Optics, USA) was employed. The PLE was measured by monochromatic light from a 300 W Xenon lamp and a high-sensitive photomultiplier tube was used as a PL detector. Time-resolved PL measurements were performed by a streak camera (Hamamatsu, C7700-01, Japan), and a mode-locked femtosecond pulsed Ti:Sapphire laser (Coherent, Chameleon Ultra II) system was used as an excitation source [400 nm (second-harmonic-generation)].

III. Results and Discussion

The oxygen composition in GOQDs and GO was investigated by X-ray photoelectron spectroscopy (XPS). The C 1s of the XPS data indicates the presence of sp^2 carbon (C-C, 284.5 eV), hydroxyl or epoxy (C-O, 286.6 eV), and carboxyl (C=O, 288.2 eV) bonds. The ratio of composition were arranged in the Table 1. The composition of GOQDs is consist of sp^2 carbon (60%), C-O (24%), and C=O (16%), whereas that of GO is consist of sp^2 carbon (46%), C-O (47%), and C=O (7%). Generally, the epoxy bonds formed on

Table 1. The C 1s of the XPS data of GOQDs and GO.

	C=C	C-O	C=O
GOQDs	60%	24%	16%
GO	46%	47%	7%

basal plane of graphene surface, and the carboxyl bonds linked at the edge of graphene. According to the XPS data, the bonds of hydroxyl or epoxy (C–O) in GO has larger composition than that of GOQDs, whereas the bonds of carboxyl (C=O) in GO has smaller composition than that of GOQDs. Because the edge to basal plane ratio of graphene increases by reducing the diameter.

The UV–vis absorbance of GOQDs and GO were measured, as shown in Fig. 1(a). The pristine graphene sheet has an absorption peak at 268.4 nm (4.62 eV) due to band–to–band transitions near the saddle–point singularity at the M–point [14]. The fabricated GO have a maximum peak of absorption at 229 nm and shoulder part at 310 nm. The absorption peak of GO is shorter wavelength than that of pristine graphene. Since the oxidation on graphene makes a number of isolated sp^2 carbon clusters in sp^3 matrix, the sp^2 carbon clusters could be affected by quantum confinement effect. To confirm recovery of properties from GO to graphene, we reduced oxygen–functional group on GO using sodium borohydride ($NaBH_4$) as a chemical reduction agent. The absorption peak at 229 nm redshifts to 265 nm, and shoulder part disappears, as shown in the Fig. 1(b). The properties of GO are similar to the results in reported literatures [15,16]. The absorption peak at 229 nm is originated from the $\pi-\pi$ transition of sp^2 carbon cluster in sp^3 matrix, and the shoulder part at 310 nm is related to $n-\pi$ transition of oxygen–functional groups. On the other hand, the GOQDs showed broad absorption with a gradual increase up to 800 nm without any absorption peaks (Fig. 1(a)). Our previous work suggested that the broad absorption of GOQDs indicates the existence of band tail by defect states [9].

The luminescent properties of GO and GOQDs were studied by PL and PLE measurement with monochromatic light from Xenon lamp, as shown in the Fig. 2(a). Irradiated by 400 nm, the PL peak position of GO exhibited a longer wavelength (~690 nm) than that of GOQDs (~520 nm). The emission from GOQDs and GO showed green color emission and red color emission. The PLE spectrum displayed the intensity of PL peak position by changing the excitation wavelengths. The PLE spectrum of GOQDs monitored at 520 nm exhibited a maximum intensity at excitation wavelength of 300 nm, whereas that of GO detected at 700 nm showed a maximum intensity at excitation wavelength of 390 nm. To further study the PL features, we measured the PL spectra by change excitation wavelengths. It has been reported that the PL peaks of GQDs, in general, redshift as excitation wavelength increases. These can be explained by their

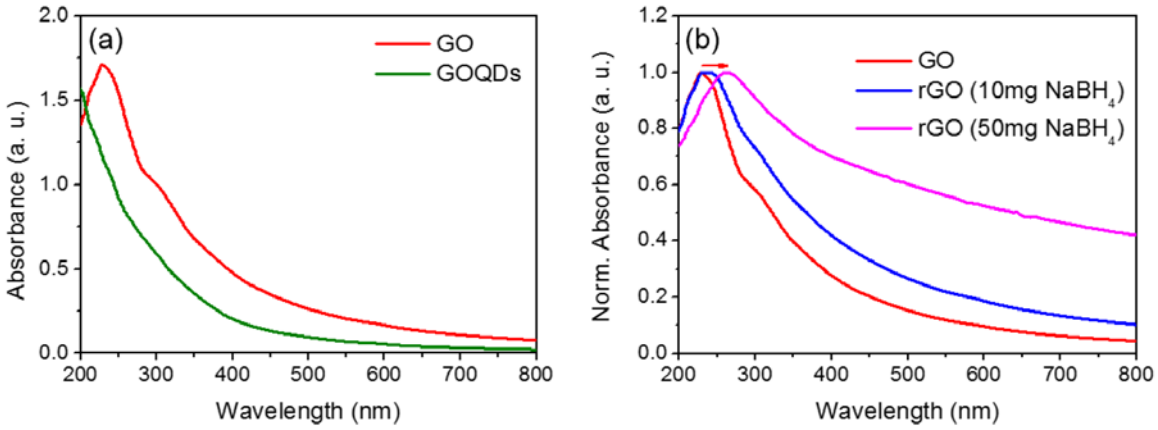

Figure 1. (a) UV–vis absorbance of GO (red line) and GOQDs (green line), (b) normalized absorbance of GO (red line), rGO prepared by 10 mg $NaBH_4$ (blue line), and rGO prepared by 50 mg $NaBH_4$ (violet line).

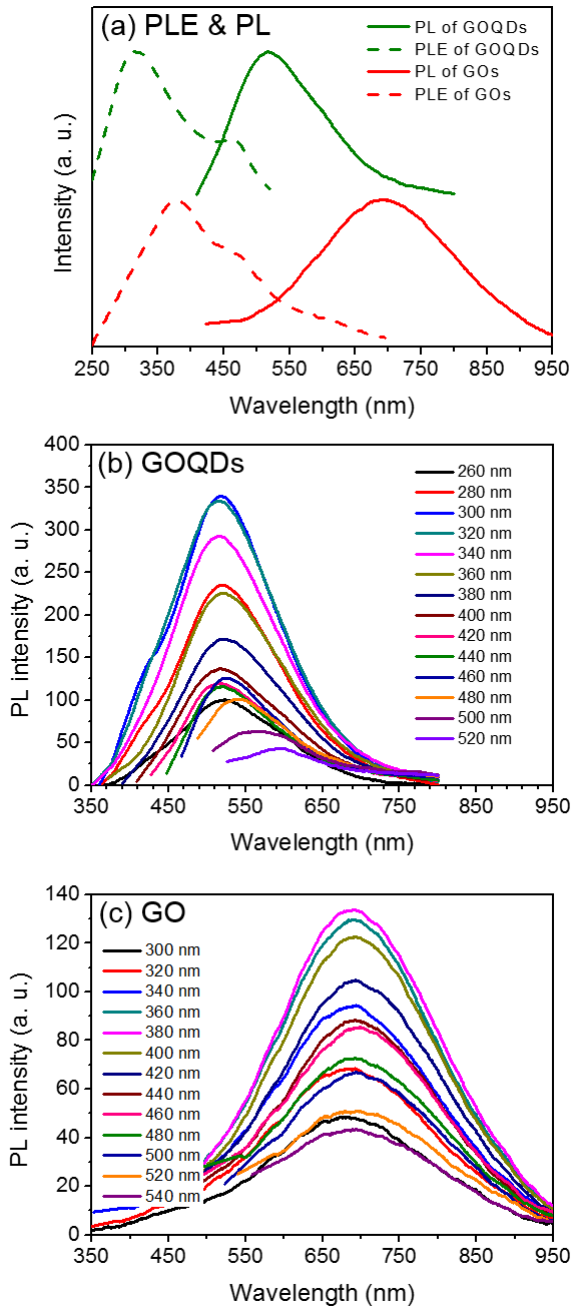

Figure 2. (a) PL (solid line) of GOQDs (green) and GO (red) irradiated by 400 nm, PLE (dash line) of GOQDs and GO detect the PL peak position at 520 nm and 700 nm, respectively, (b) and (C) PL spectra of GOQDs and GO under various excitation wavelengths.

inhomogeneous size distributions and defect states. However, the GO showed invariant PL emission at 690 nm under various excitation wavelengths from 300 nm to 540 nm (Fig. 2(c)). In the case of the GOQDs, as

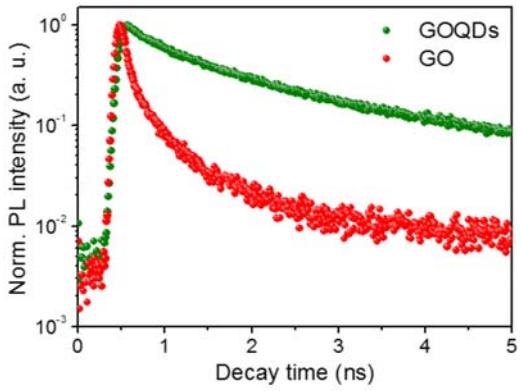

Figure 3. PL decay profile of GOQDs (green) and GO (red).

shown in the Fig. 2(b), the PL emission kept at 510 nm by changing excitation wavelengths from 260 nm to 460 nm and redshifted after 480 nm of excitation wavelength.

To understand the recombination process of GO and GOQDs, we performed time-resolved PL using a femtosecond Ti:Sapphire laser and a streak camera detector. The time-resolved PL of GO and GOQDs were measured irradiated by 400 nm pulse source. Fig. 3 shows the PL decay profile of GOQDs (green circle) and GO (red circle), which were extracted from all spectrum detected by streak camera (Fig. 4). The lifetimes of GO and GOQDs, which were estimated as the time when an intensity decreases to 1/e of the maximum, are 0.13 ns and 0.95 ns, respectively. Our previous work has reported that the fast decay time could be observed in GQDs with sp^2 carbon domain [9,10]. To further study their carrier dynamics, we plotted the time-dependent integral PL (TIPL), which exhibits the temporal spectrum profile as time passes. As shown in Fig. 4(a), upon a time delay, the temporal spectra of the GOQDs show an invariable PL behavior. It is considered that the presence of only one PL origin originated from the extrinsic states of the oxygen-functional groups [10]. Since the GOQDs have smaller than 4 nm (GNPs), it is difficult to obtain isolated sp^2 carbon cluster. After reduction process, the PL behavior from the isolated sp^2 carbon

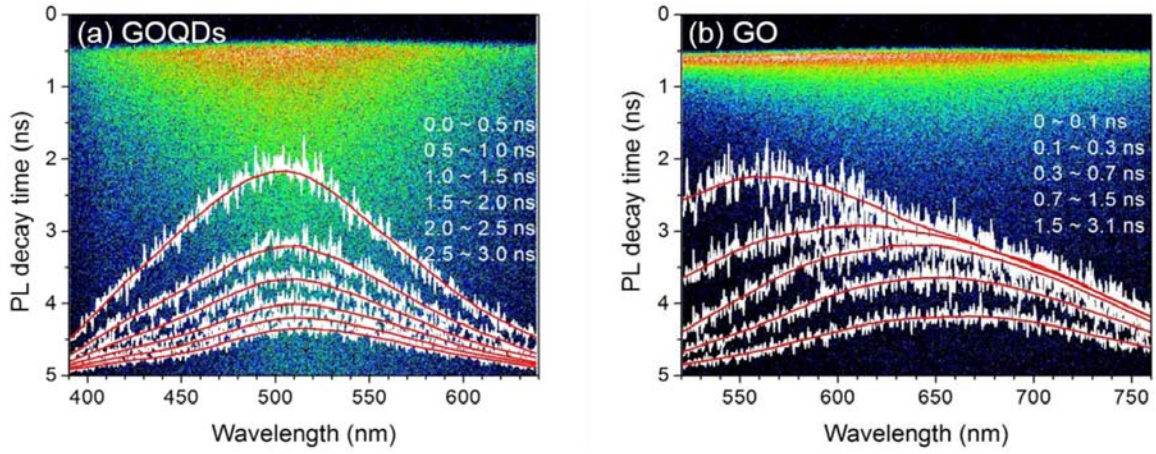

Figure 4. The time-dependent integral PL spectra from the GOQDs (a) and GO (b) under excitation at 400 nm by a second harmonic-generation femtosecond pulse laser.

cluster in the GOQDs could be observed [10]. On the other hand, the PL spectra of the GO redshifted from 560 nm to 660 nm after the pump event (Fig. 4(b)). This result is very similar to optical properties of reduced GOQDs (rGOQDs) with sp^2 carbon nano-sized cluster [10]. Chien et al. observed isolated small sp^2 clusters with ~2 nm around sp^3 bonding in GO, which have broad red PL emission [17]. However, they didn't observe the change of PL spectra upon a time delay. From our TIPL result, we could suggest that the PL at 560 nm with fast decay time is originated from intrinsic states of small sp^2 clusters with ~2 nm, whereas the PL at 660 nm with slow decay time is derived from extrinsic states of oxygen-functional groups.

IV. Conclusions

The optical properties of GO and GOQDs have been studied by means of PL, PLE, UV-vis absorbance, and time-resolved PL. Both samples have broad absorption due to oxygen-functional group on graphene. The GO have an absorption peak at 229 nm and shoulder part at 310 nm, whereas the GOQDs show broad absorption with a gradual change up to 800 nm without any absorption peaks. The PL emission of GOQDs and GO showed the green color at 520 nm and the red color at 690 nm, respectively. The red emission of GO showed fast PL decay time than the green emission of GOQDs. In particular, the temporal PL profile of the GO have shown redshift trend 560 nm to 660 nm after the pump event, suggesting that luminescence origins in the GO have two types of the intrinsic states of small sp^2 clusters with ~2 nm and extrinsic states of oxygen-functional groups.

Acknowledgements

This work was supported by the graphene research center (GRC) project of KI for the NanoCentury.

References

[1] A. K. Geim, Science **324**, 1530 (2009).

[2] T. Gokus, R. R. Nair, A. Bonetti, M. Böhmler, A. Lombardo, K. S. Novoselov, A. K. Geim, A. C. Ferrari, and A. Hartschuh, ACS Nano **3**, 3963 (2009).

[3] D. Pan, J. Zhang, Z. Li, and M. Wu, Adv. Mater. **22**, 734 (2010).

[4] J. Shen, Y. Zhu, X. Yang, and C. Li, Chem. Commun. **48**, 3686 (2012).

[5] H. Sun, L. Wu, W. Wei, and X. Qu, Materials Today **16**, 433 (2013).

[6] J. Peng, W. Gao, B. K. Gupta, Z. Liu, R. R. Aburto, L. Ge, L. Song, L. B. Alemany, X. Zhan, G. Gao, S. A. Vithayathil, B. A. Kaipparettu, A. A. Marti, T. Hayashi, J. J. Zhu, and P. M. Ajayan, Nano Lett. **12**, 844 (2012).

[7] S. Kim, S. W. Hwang, M. K. Kim, D. Y. Shin, D. H. Shin, C. O. Kim, S. B. Yang, J. H. Park, E. Hwang, S. H. Choi, G. Ko, S. H. Sim, C. Sone, H. J. Choi, S. Bae, and B. H. Hong, ACS Nano **6**, 8203 (2012).

[8] S. H. Song, M.-H. Jang, J. Chung, S. H. Jin, B. H. Kim, S.-H. Hur, S. Yoo, Y.-H. Cho, and S. Jeon, Adv. Optical Mater. **2**, 1016 (2014).

[9] F. Liu, M.-H. Jang, H. D. Ha, J.-H. Kim, Y.-H. Cho, and T. S. Seo, Adv. Mater. **25**, 3657 (2013).

[10] M.-H. Jang, H. D. Ha, E.-S. Lee, F. Liu, Y.-H. Kim, T. S. Seo, and Y.-H. Cho, Small 2015, DOI: 10.1002/smll.201500206.

[11] S. Umrao, M.-H. Jang, J.-H. Oh, G. Kim, S. Sahoo, Y.-H. Cho, A. Srivastva, and I.-K. Oh, Carbon **81**, 514 (2015).

[12] F. Liu, and T. S. Seo, Adv. Funct. Mater. **20**, 1930 (2010).

[13] H. D. Ha, M.-H. Jang, F. Liu, Y.-H. Cho, and T. S. Seo, Carbon **81**, 367 (2015).

[14] K. F. Mak, J. Shan, and T. F. Heinz, Phys. Rev. Lett. **106**, 046401 (2011).

[15] D. Li, M. B. Müller, S. Gilje, R. B. Kaner, and G. G. Wallace, Nat. Nanotech. **3**, 101 (2008).

[16] U. Lange, T. Hirsch, V. M. Mirsky, and O. S. Wolfbeis, Electrochimica Acta **56**, 3707 (2011).

[17] C.-T. Chien, S.-S. Li, W.-J. Lai, Y.-C. Yeh, H.-A. Chen, I-S. Chen, L.-C. Chen, K.-H. Chen, T. Nemoto, S. Isoda, M. Chen, T Fujita, G. Eda, H. Yamaguchi, M. Chhowalla, and C.-W. Chen, Angew. Chem. Int. Ed. **51**, 6662 (2012).